Journal of Solar Energy Research (JSER)

Journal homepage: www.jser.ut.ac.ir

Solar Photovoltaic and Wind Turbine Generation based Microgrid Management Architecture Considering Battery Energy Storage Degradation and Time of Use Tariff

Samarjit Patanik[a, *], Neelakantha Guru[b], Kumari Kasturi[c], Manas Ranjan Nayak[b]

[a]*Department of Electrical Engineering, Odisha University of Technology and Research, Odisha, India.*
[b]*Department of Electrical Engineering, Biju Patnaik University of Technology, Odisha, India.*
[c]*Department of Electrical Engineering, Siksha 'O' Anusandhan University, Odisha, India.*

ARTICLE INFO

Article Type:
Original Article

Received:03.03.2023
Accepted:19.04.2023

Keywords:
Photovoltaic
Energy management
Wind turbine generation
Artificial Rabbit Optimisation
State of health

A B S T R A C T

The rapid expansion of renewable energy sources (RES), especially the combination of solar photovoltaic (PV), wind turbine generating (WTG), and battery energy storage systems (BESS), has sparked significant interest in addressing global warming and climate change issues. These energy sources offer numerous advantages, such as reduced emissions and lower operational costs, but their power output is uncertain. In order to account for fluctuating energy costs, a microgrid with diverse energy sources must schedule BESS charging optimally. The proposed method uses the Artificial Rabbit Optimisation (ARO) algorithm to optimise the charging and discharging schedule for BESS, resulting in a decrease in daily energy costs and an improvement in storage state of health (SOH). The SOH is considered an ageing coefficient for conservative BESS operation in order to extend the battery's lifespan under consistent use. To further validate the effectiveness of the energy management strategy, a fixed pricing scheme and a dynamic pricing scheme are utilised to validate its efficacy. When storage degradation and time-of-use (TOU) tariffs are accounted for, the simulation results of voltage, current, and power profiles over a 24-hour period indicate that the proposed method has the capability to maximise the profitability of a grid-connected PV and WTG-based microgrid.

1. Introduction

Recent studies show that coal, oil, and gas, the three main energy sources, make up about 75% of the

*Corresponding Author Email:patnaik.samarjit@outr.ac.in

Cite this article: Patanik, S., Guru, N., Kasturi, K., & Nayak, M. (2023). Solar Photovoltaic and Wind Turbine Generation based Microgrid Management Architecture Considering Battery Energy Storage Degradation and Time of Use Tariff. Journal of Solar Energy Research, 8(2), 1459-1470.

DOI: 10.22059/jser.2023.356135.1276 DOR: 20.1001.1.25883097.2023.8.2.9.7

world's energy. However, these energy sources emit a great deal of carbon, which is harmful to the air, rain, land, and human health. In addition, traditional fossil fuels are being depleted rapidly and cannot meet the rising demand for global energy. Renewable energy sources (RES), a viable alternative to conventional resources, can be utilised to accomplish the green energy requirement for sustainable development as per Elavarasan et al. [1]. RES, such as solar and wind, can generate electricity without emitting greenhouse gases. They have become more prevalent and cost-effective, and their use in existing power systems has increased. However, the energy production of RES sources is highly dependent on climate and weather variations as per Solaun et al. [2]. These sources must be integrated with other stable energy sources, such as fuel cells, microturbines, battery storage, etc., to ensure a constant supply of high-quality energy as per Sarwar et al. [3]. These hybrid systems are effective as sources of sustainable energy.

In this situation, the microgrid is helpful because it saves energy and works with a wide range of renewable energy sources (RES). Blesslin et al. [4] discussed, microgrids can meet local capacity needs and connect to or disconnect from the utility grid by using different types of distributed renewable energy sources (RES). Microgrids (MGs) can operate independently or in tandem with the main grid. (i.e., as islands). Therefore, MGs are able to generate, distribute, and regulate electricity for remote consumers as per Ishaq et al. [5]. It is believed that microgrids (MGs) facilitate a high penetration of renewable energy sources (RES) in power grids. Large penetrations of distributed RES necessitate the creation of innovative dispatch systems in order to balance generation and demand as discussed in Kumar et al. [6]. A hierarchical architecture incorporates and maintains dispersed energy storage technologies for reliability and energy security discussed by Shahgholian [7]. High penetration of RES can lead to power imbalances, especially for residential single-phase consumers studied by Jabalameli and Ghosh [8]. MGs are necessary for future intelligent grids, which could transform centralised electrical networks into distributed designs.

Over the past years, researchers have endeavoured to create an effective hybrid system to mitigate the issues associated with RES. The authors propose a multi-agent consensus-distributed control strategy devised to achieve multiple objectives for the placement and sizing of RES simultaneously as per Kandari et al. [9]. The consensus-distributed multi-agent control strategy considers the frequency/voltage droop controllers and hierarchical control architecture of the battery energy storage system (BESS). Zarei and Ghaffarzadeh present a multi-objective optimisation of the AC optimal power flow (AC-OPF) problem in terms of demand response (DR) [10]. The objective of the work by Mirzkhani and Pishkar [11] is to attain peak reduction and valley filling for active and reactive power, as well as to minimise total voltage deviation and system cost. This study by Aryan [12] investigated the effects of wind speed variations on optimal configuration and planning for a hybrid renewable energy system. The impact of changes in wind speed on the annual production of wind turbines, cost of energy, net present cost, and fuel consumption was determined. This study by Ghaffarzadeh and Faramarzi [13] discussed about identifying the optimal location for solar photovoltaic (SPV) facilities to improve energy efficiency by minimising losses and enhancing voltage profiles. Using the holomorphic load flow algorithm and the particle swarm optimisation (PSO) algorithm, the multi-objective function is converted to a single-objective function.

A number of articles have described use of metaheuristic algorithms for optimal size of hybrid renewable energy system. An interesting model named mixed integer linear programming (MILP) was presented by Theo et al. [14]. Logesh [15] discussed soft computing methods for energy management and power flow management in presence of hybrid system. Fathima and palanisamy [16] presented a detailed survey on otimization in hybrid systems. Gamarra et al. [17] discussed computational optimization for microgrid. Over time, a battery's performance diminishes; monitoring data may be utilised to evaluate the battery's true health condition. A comparative analysis of battery ageing and capacity loss / impedance growth has been various economic reduction strategies for energy management in systems that include SOH discussed by Sarker et al. [18]. Parvin et al. [19] discuss technologies for energy-efficient power grids. A comprehensive analysis was conducted that accounted for the numerous challenges associated with smart-grid demand-side management. The first two levels of the demand-side load management architecture are thought to be line planning and low-cost scheduling. Demand response is a third-level subject that has been studied a lot in the last ten years.This study looks at whether or not it is possible

to change the way consumer products are set up in order to meet the needs of the distribution system when it is overloaded. Khezri and Mahmoudi [20] argue that there is a trade-off between minimising energy consumption and maximising user convenience because existing scheduling systems do not account for user activities. By directly incorporating user actions into a proposed load-optimisation technique, the trade-off between user convenience and electricity cost was diminished. This trade-off was considered, and optimisation models were developed and implemented for a variety of household appliances. The results of the simulation were evaluated in terms of occupancy, cost, and decrease in energy utilisation.

Few studies have examined the optimal placement of the BESS and the ability of wind turbine generation (WTG) to penetrate, in addition to their own processes and characteristics as discussed by Patnaik et al. [21]. For scheduling RESs, a novel stochastic multi-area unit commitment architecture is utilised. In order to improve the resiliency, a method proposed by Kunya et al. [22] based on peak load shaping, ramping-up and ramping-down rates of load, and the spread of uncertainty factors are evaluated. Zeng et al. [23] investigated the probable relationships between RES uncertainty and a price-based demand response programme. Chen et al. [24] have proposed a realistic scheduling model of grid-connected microgrids based on chance-constrained programming to minimise operating costs and improve the user experience by formulating the unpredictability of renewable generation output. Moreover, a metric for measuring user satisfaction was devised from the view of demand-side management.

In the course of research, a variety of techniques have been employed to address complex power system optimisation issues as discussed by Jordehi [25]. To address rapid convergence, vast search spaces, and multi-objective optimisation functions, swarm-based algorithms inspired by biology have been developed and studied by Tian et al. [26]. However, there is no single optimisation algorithm that can overcome all obstacles. The no free lunch (NFL) theorem explains why new bio-inspired optimizers are constantly being created despite the fact that so many already exist as per Adam et al. [27]. This study is motivated by the NFL theorem, which encourages the development of more efficient bio-inspired optimizers. In addition, the majority of optimizers feature multiple control alternatives as per Rodríguez-Molina et al. [28]. This article introduces the artificial rabbit optimisation (ARO) algorithm, which was inspired by the survival strategies of rabbits in the open and their detour foraging and unpredictable hiding behaviours as discussed in Wang et al. [29]. ARO is exceptionally competitive in the resolution of difficult engineering optimisation problems.

Even though there have been numerous studies of BESS coupled with wind for grid-level peak load regulation as described by de Siqueira and Peng [30]. These studies have focused on small-scale BESS and encompassed a portion of a grid's total wind output or implemented wind-BESS systems primarily to maximise financial metrics as per Yang et al. [31]. The scope of research has not been restricted to PV/WTG-BESS scheduling for the enhancement of storage health. Such research is required to perceive the techno-economic-environmental potential of PV and WTG based BESS micro-grid operating issues and their potential profitability while integrating with the national grid. This article employs artificial rabbit optimisation (ARO) to determine the optimal battery charging and discharging schedule for a grid-connected microgrid with RES sources. The most significant contributions to this work are:

1. To investigate a multi-objective operational strategy for a microgrid with multiple renewable energy sources and battery energy storage for maximising consumer benefit.
2. Scheduling the charging and discharging of BESS from the grid as necessary, and ensuring the transaction of surplus power generated by renewable sources to the grid.
3. The energy price has a greater variation between on-peak and off-peak charges and the effect of different pricing schemes on operational strategy is analysed.
4. Ensuring consumer profit and simultaneously enhancing battery state of health.

The remaining portions of the paper are organised as follows: The second component concerns mathematical modelling. Section 3 outlines the objective of the study. Section 4 discusses the ARO algorithm. Section 5 illustrates and analyses results. Lastly, section 6 concludes the article.

2. Materials and Methods

2.1. Modelling of the system

Figure 1 depicts the fundamental structure of an energy management system (EMS). The system comprises PV, WTG, BESS, the grid, charge

controllers, converters, and user loads. The principal function of EMS is to regulate power transmission in the microgrid. The BESS must provide and receive power for maximising user benefits during discharge and charging, respectively. In order to ensure the reliability of the power system, the system must be capable of delivering electricity on demand.

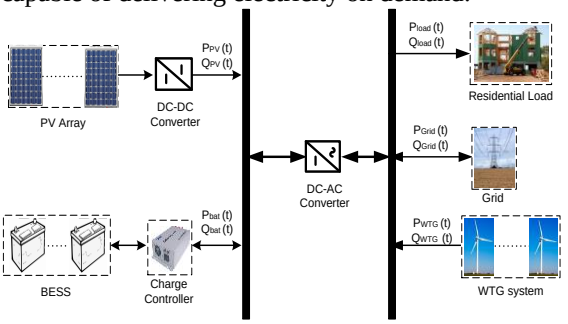

Figure 1. System overview

2.1.1. PV system modelling

A solar cell's ability to convert photon energy into clean power when linked in series and parallel makes it an essential part of a PV module. Clean, renewable energy is generated when these modules are connected to form PV arrays. Each solar cell functions as a component in a larger electrical system. The mathematical expression for the power generated by a PV panel as a function of solar irradiance is [32].

$$P_{PV}(t) = \begin{cases} P_{rated_{PV}}\left(\frac{R^2}{R_{STD} * R_C}\right), & R < R_C \\ P_{rated_{PV}}\left(\frac{R}{R_{STD}}\right), & R_C \le R < R_{STD} \\ P_{rated_{PV}}, & R > R_{STD} \end{cases} \quad (1)$$

Where $P_{rated_{PV}}$= 5 kW, $R_{STD} = 1000\, W/m^2$ and $R_C = 150\, W/m^2$. The hourly solar irradiation data for the selected day is gathered from Indian Meteorological Department (IMD) [33]as per Figure 2. The most solar power is made between 10 AM and 2 PM, when the sun shines the brightest.

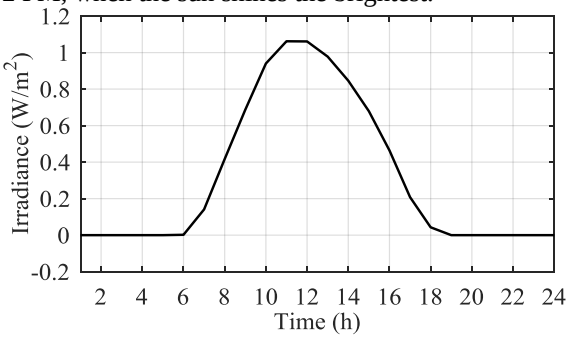

Figure 2. Mean hourly solar irradiance in a day

2.1.2. Modelling of the WTG system

The Power output of WTG ($P_{WTG}(t)$) is calculated as follows[34].

$$\begin{cases} 0, & v(t) < v_{cin} \\ \frac{1}{2}\rho A_s v^3(t)\eta_{wd}\eta_{conv}N_W, & v_{cin} \le v(t) \le v_{rd} \\ P_{wd_{max}}N_W, & v_{rd} \le v(t) \le v_{cout} \\ 0, & v(t) > v_{cout} \end{cases} \quad (2)$$

Here, air density is calculated as follows:

$$\rho = \frac{P.\ MW}{R(273.15+T_a)} \quad (3)$$

Where MW is the Molecular weight. Wind speed data in Bhubaneswar was collected from IMD [33]as per Figure 3. The wind power variation is between 0.9 m/sec to 4 m/sec throughout the day.

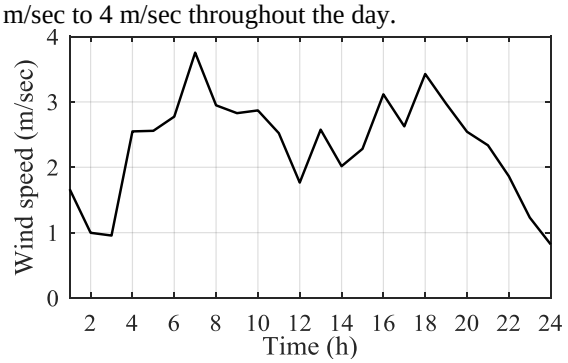

Figure 3. Hourly Wind speed in a typical day

The wind turbine specifications are illustrated in Table 1.

Table 1. Wind turbine Specifications [33]

Name of the Parameter	Specification
Number of wind turbines	1
Swept area of wind turbine	41.1 m^2
Pressure in atm	1 atm
Ambient temperature	27 $^\circ C$
Wind Turbine efficiency	30%
Converter efficiency	95%
Maximum Output Power in kW	1.4 kW
Ideal gas constant	8.025×10^{-5} m^3atm $K^{-1}mol^{-1}$
Cutin speed	2 m sec^{-1}
rated speed	9.5 m sec^{-1}
cutout speed	12 m sec^{-1}

2.1.3. Modelling of BESS

The Lead Acid Battery of Rolls-Surette S-550 make and Flooded Deep Cycle type are considered

for this study. The voltage during charging and discharging of BESS is calculated as per eqn (5) and (6) based on the linear interpolation [35]. The voltage and current of the BESS depend upon the schedule of SOC and the output power is formulated [33] as per eqn (4).

$$P_{bat}(t) = V_{bat}(t)\, I_{bat}(t) \quad (4)$$

$$V_{bat}(t) = [6.75 + 1.2SOC(t)]N_{bat}(t), \quad I_{bat} > 0 \quad (5)$$

$$V_{bat}(t) = \left[6.29 - 1.02\left(1 - SOC(t)\right)\right]N_{bat}(t), \quad I_{bat} \le 0 \quad (6)$$

Where, $V_{bat}(t)$ is the voltage of battery, $N_{bat}(t)$ represents the batteries linked in series and state of charge is represented as SOC (t). The floating voltage of each battery is 6.75 V and 4 batteries are considered in series with total capacity of BESS as 400 Ah. The battery current $I_{bat}(t)$ and SOH are calculated as per eqn (7), (8), (9).

$$I_{bat}(t) = \frac{\Delta Q}{dt} \quad (7)$$

$$\Delta Q = C(t) - C(t - \Delta t) = C_{x_k} - C_{x_j} \quad (8)$$

$$SOH(t) = \frac{C_r(t)}{C_{r,nom}(t)} \quad (9)$$

where $C_{r,nom}(t)$ is the nominal capacity [19]. According to [36] and [36, 37], the battery performance degrades with each discharge in this model. According to [38], capacity of reference losses is regarded as linearly dependent on battery depletion. If the change in SOC is smaller than zero at each change in time, the BESS is in discharging mode, then the reference capacity is computed by (13) and (14).

$$C_r(t) = C_r(t - \Delta t) - \Delta C_r(t) \quad (10)$$

$$\Delta C_r(t) = C_{r,nom}(t)\, Z\, [SOC(t - \Delta t) - SOC(t)] \quad (11)$$

Where, Z = 0.00031 is the ageing coefficient. The minimum and maximum SOC levels are 20% and 90% with permissible step change in SOC at 1%.

2.1.4. Modeling of Load

For a specified day of summer, at Bhubaneswar, the power consumption of residential utility customers was used to create the hourly load profile data displayed in Figure 4. The average load during the day is 1.224 kW with peak load of 1.604 kW during 11th and 19th hours and lowest demand of 0.70 kW at 4th hour of the day.

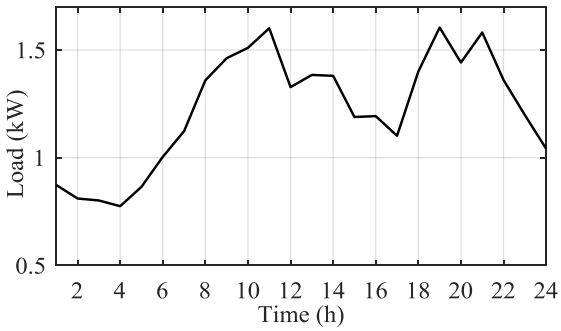

Figure 4. Load profile in a day

2.1.5. Modeling of Grid

The energy management determines how much energy must be produced to meet demand and how much energy must be stored in the battery. If natural resources provide little or no energy, the microgrid relies on the grid. If there is surplus electricity, the microgrid supplies it to electrical grid.

In case of power received and transferred to the grid as per eqn (15) and (16):

$$P_{Grid}(t) = P_{Load}(t) - P_{PV}(t) - P_{WTG}(t) \mp P_{bat}(t),\ P_{Grid} < 0 \quad (12)$$

$$P_{Grid}(t) = P_{Load}(t) - P_{PV}(t) - P_{WTG}(t) \mp P_{bat}(t),\ P_{Grid} \ge 0 \quad (13)$$

The energy pricing for Fixed and Time-of-Use types are considered in the study. The Electricity Grid Price (EGP) and Feed-In Tariff (FIT) are formulated as per Table 2.

Table 2. Electricity pricing during the day [39]

Type of price	Time of a day	EGP (Rs/kWh)	FIT (Rs/kWh)
Tier 1	All hours	4.00	4.00
Tier 2	Off-Peak hours [1-10, 23-24]	2.50	1.50
	Peak hours [11-22]	3.50	6.00

2.2. Problem definition

The objective considers the energy received or supplied to the grid at any given time, and the capturing the degradation of BESS state of health as the ageing cost, incorporating the operating constraint.

2.2.1. Objective

The minimization of the objective of the system may be stated as:

$$F_{obj} = \sum_{t=t_0}^{T} \left(C_R(t) + C_P(t)\right) \quad (14)$$

where F_{obj} is the total cost including cash outflow and cash inflow for a day, $C_R(t)$ is the cash outflow and $C_P(t)$ is the cash inflow. The cost is computed for each time step, as per (18).

$$F_{obj}(\Delta t) = \left(C_R(\Delta t) + C_P(\Delta t)\right) \quad (15)$$

The cash outflow and cash inflow are computed as:

$$C_P(\Delta t) = P_{Grid}(\Delta t)EGP(\Delta t) + BrC(\Delta t), \quad P_{Grid}(\Delta t) \geq 0 \quad (16)$$

$$C_R(\Delta t) = P_{Grid}(\Delta t)FIT(\Delta t), \quad P_{Grid}(\Delta t) < 0 \quad (17)$$

where *EGP* and *FIT* are as per Table 2.

The ageing cost for BESS (BrC) is determined by[39]:

$$BrC(t) = \frac{BiC\left(-\Delta SOH(t)\right)}{1 - SOH^{min}} \quad (18)$$

Where BiC represents the investment cost for the BESS at Rs 9125 per kWh.

2.2.2. System Operating Constraints

The system works within the confines of the following limits on equality and inequity.

$$P_{Grid}(t) = P_{load}(t) - P_{PV}(t) - P_{WTG}(t) \mp P_{bat}(t) \quad (19)$$

$$SOC^{min} \leq SOC(t) \leq SOC^{max} \quad (20)$$

$$P_{bat}^{min} \leq P_{bat}(t) \leq P_{bat}^{max} \quad (21)$$

$$SOH(t) \geq SOH^{min} \quad (22)$$

$$P_{Grid}(t) \leq P_{Grid}^{max} \quad (23)$$

$$\Delta SOC^{min} < \Delta SOC(t) \leq \Delta SOC^{max} \quad (24)$$

Eqn (19) specifies the laws of power conservation, eqns (20) – (22) & (24) protects the BESS from health degradation owing to excessive charging and high depth of battery depletion, and limits the battery's degradation; in eqn (23) the grid power must not exceed the maximum limit; otherwise, penalty cost is imposed in the calculation of cash flow.

2.3. Artificial Rabbits Optimisation Algorithm

Artificial rabbit optimization (ARO) is a novel bio-inspired algorithm that takes cues from rabbits' strategies for survival to tackle the challenging issue of nonlinear optimization [29]. The ARO algorithm was developed with inspiration from survival strategies including foraging and hiding in unexpected places. Such survival strategies are mathematically illustrated in this study.

a) Detour foraging

Rabbits do not bother with nearby food sources while they are foraging. It is called "detour foraging" because they never eat grass from their own yards, but rather ingest it at random from other areas. It is assumed that each candidate in the colony has its own area, having food and d burrows, and that the candidates graze at random between themselves. The fact is that rabbits will hunt around in the ground to find enough to eat. ARO's detour foraging behaviour shows that each search candidate would rather update its position in relation to a different, randomly chosen search individual in the swarm in order to create a diversion. Detour foraging by rabbits is modelled mathematically as follows:

$$\vec{V}_i(t+1) = \vec{x}_j(t) + R\left(\vec{x}_i(t) - \vec{x}_j(t)\right) + \text{round}\left(0.5\left(0.05 + r_1\right)\right)n_1 \quad (25)$$

$$R = L\,c \quad (26)$$

$$L = \left(e - e^{\left(\frac{t-1}{T}\right)^2}\right)\sin(2\pi r_2) \quad (27)$$

$$c(k) = \begin{cases} 1 & \text{if } k == g(l) \\ 0 & \text{else} \end{cases} \quad (28)$$

$$g = \text{randperm}(d) \quad (29)$$

$$n_1 \sim N(0,1) \quad (30)$$

where $\vec{V}_i(t)$ indicates position of the i^{th} candidate at instant t, n indicates number of the rabbits, d signifies the dimension, T denotes the number of iterations, $c(k)$ denotes the ceiling function, randperm generates integers in range of 1 to d, r_1, r_2, randomly and eqn (28) suggests that search people conduct a random search for food based on their relative positions. This habit enables a rabbit to travel to the territories of others irrespective of distance. The unique foraging behaviour adds to exploration and ensures the ARO algorithm's global search capacity.

b) Random hiding

A rabbit will create a complex network of tunnels around its den to hide it from potential predators. To decrease its chances of getting eaten, a rabbit in ARO always constructs d burrows along the search space at each iteration and chooses a tunnel at random for hiding. The following formula is provided as a result of this:

$$\vec{b}_{i,j} = \vec{x}_i(t) + H\, g\, \vec{x}_i(t)) \quad (31)$$

$$H = \frac{T - t + 1}{T}\, r_4 \quad (32)$$

$$n_2 \sim N(0,1) \quad (33)$$

$$g(k) = \begin{cases} 1 & \text{if } k == g(l) \\ 0 & \text{else} \end{cases} \quad (34)$$

Based on eqn (34), d burrows are constructed. H represents the parameter for hiding, which is lowered in a range of 1 to $\frac{1}{T}$ with a random perturbation throughout the duration of repetitions. As stated before, rabbits are often pursued and attacked by predators. To live, candidates must occupy a secure hiding spot. Therefore, they are not permitted to randomly choose a tunnel from among their burrows in order to prevent being captured. To formally represent this random concealment technique, the subsequent equations are proposed:

$$\vec{V}_i(t+1) = \vec{x}_i(t) + R\left(r_4\, \vec{b}_{i,r}(t) - \vec{x}_i(t)\right) \quad (35)$$

$$g_r(k) = \begin{cases} 1 & \text{if } k == [r_5 \;\; d] \\ 0 & \text{else} \end{cases} \quad (36)$$

$$\vec{b}_{i,r}(t) = \vec{x}_i(t) + H\, g_r\, \vec{x}_i(t) \quad (37)$$

where $\vec{b}_{i,r}(t)$ denotes the direction of burrow for hiding, r_4 and r_5 , represent integers in range of (0,1). The i^{th} rabbit updates its position towards the burrow. The location of the rabbits is updated as per eqn (38):

$$\vec{x}_i(t+1) = \begin{cases} \vec{x}_i(t) & f(\vec{x}_i(t)) \le f\left(\vec{V}_i(t+1)\right) \\ \vec{V}_i(t+1) & f(\vec{x}_i(t)) > f\left(\vec{V}_i(t+1)\right) \end{cases} \quad (38)$$

c) Energy shrink

In ARO, rabbits usually do detour foraging during the early phase of iterations, but they commonly practice random hiding during the final phase. This search mechanism is powered by the energy of a candidate, which will diminish subsequently over a period. Consequently, an energy is created to simulate the transition. The factor A(t) is evaluated as follows:

$$A(t) = 4\left(1 - \frac{t}{T}\right)\ln\frac{1}{r} \quad (39)$$

Here r is an arbitrary value in the range of (0,1). The high energy factor value indicates that the individual has adequate energy for detour foraging. Whereas, the low value of the energy component suggests that a candidate is less physically active, and hence requires arbitrary concealment. ARO may switch between detour foraging and arbitrary concealment according to the value of the component A. Exploration happens for $A(t) > 1$, whereas exploitation occurs if $A(t) \le 1$. To explore the effect of the energy factor on the algorithm's search behaviour, the probability of A > 1 is computed as:

$$P\{A(t)\} = \frac{1}{4}\int_0^{-\frac{1}{4}} \frac{e^t}{t}\, dt + e^{-\frac{1}{4}} \quad (40)$$

Therefore, the likelihood of detour foraging throughout the repeated procedure is around 0.5. The algorithm does almost equal amounts of detour foraging and arbitrary concealment in iterative phase, as it greatly contributes to managing exploration and exploitation. The search behaviors in ARO are determined by the range of A, which steadily rises with the increase in random oscillator rounds. Contrary to it, the declining pattern of A compels the ARO to execute exploration often in the early iterations and exploitation frequently in the latter iterations. This also helps the ARO transition gradually from global to local search. The random oscillator, on the other hand, does not alter the declining pattern of A, which initially leads to exploration and eventually exploitation. In the meanwhile, the factor A enables exploration in the algorithm's last phases of iteration.

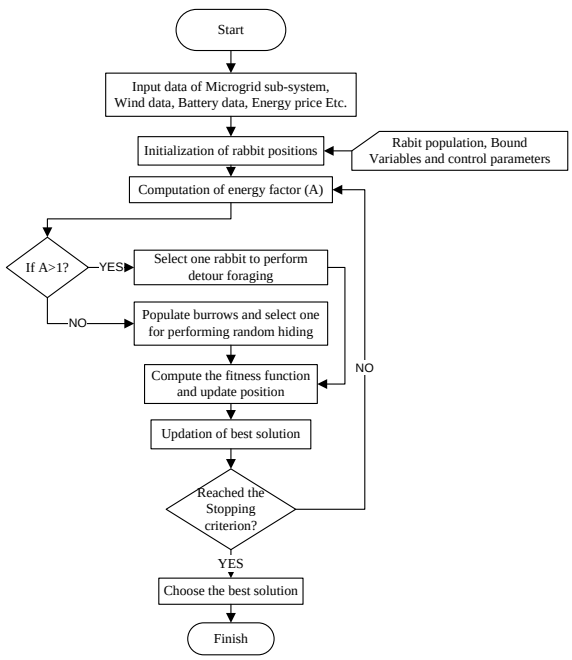

Figure 5. Flowchart of ARO algorithm

Collectively, the ARO algorithm generates a random population of initial solutions in the search space. At each cycle, an individual changes its location relative to either a randomly selected individual from the generation or one from its burrows. As the number of iterations increases, the energy factor A decreases, causing rabbits in the population to alternate between exploration phase and exploitation phase. All updates and calculations are

performed interactively until the termination requirement is reached, at which point the best solution is returned. The flowchart is shown in Figure 5.

3. Validation

To evaluate the performance of the ARO to that of other algorithms, a series of simulations were done. Table 3 describes four uni-modal benchmark functions for assessing the performance index.

Table 3. Function declaration

Function	Definition	Range
$F_1(x)$	$\sum_{i=1}^{n} x_i^2$	$[-100, 100]^n$
$F_2(x)$	$\sum_{i=1}^{n} \left(\sum_{j=1}^{i} x_j\right)^2$	$[-100, 100]^n$
$F_3(x)$	$\sum_{i=1}^{n-1} (100(x_{i+1} - x_i)^2) + (x_i - 1)^2$	$[-30, 30]^n$
$F_4(x)$	$\sum_{i=1}^{n} (ix_i^4 + \text{random}[0,1])$	$[-1.28, 1.28]^n$

This assessment of the performance of the optimization technique depends on the evaluation of 30 separate runs comprising 500 iterations each. It was calculated and compared the standard deviation, the mean error, and the best error.

Table 4 (a). Results of performance metric comparison

Function	Parameter	GSA	TLBO	ARO
$F_1(x)$	Mean	2.19E−17	3.64E−87	1.82E−124
	Stdev	6.38E−18	1.67E−88	6.63E−124
	Best	1.15E−17	1.53E−89	2.29E−142
$F_2(x)$	Mean	2.22E+02	5.65E−17	1.24E−95
	Stdev	7.07E+01	2.28E−17	6.78E−94
	Best	8.53E+01	4.02E−19	7.00E−115
$F_3(x)$	Mean	2.22E+02	2.14E+01	4.55E−03
	Stdev	7.07E+01	1.11E+00	5.12E−03
	Best	8.53E+01	1.76E+01	2.41E−04
$F_4(x)$	Mean	1.91E−02	5.62E−04	2.51E−04
	Stdev	6.87E−03	1.72E−04	1.07E−04
	Best	7.73E−03	1.47E−04	6.28E−05

Table 4 (a) and (b) compares the performance characteristics of Gravitational search algorithm (GSA), Teaching-learning-based optimization (TLBO) method, Particle swarm optimization (PSO), Differential evolution (DE), and ARO. As seen in the table, ARO yields superior outcomes compared to other optimization techniques.

Table 4 (b). Results of performance metric comparison

Function	Parameter	PSO	DE	ARO
$F_1(x)$	Mean	2.15E−04	3.64E−14	1.82E−124
	Stdev	2.25E−04	6.06E−14	6.63E−124
	Best	2.99E−06	1.26E−15	2.29E−142
$F_2(x)$	Mean	2.84E+03	5.69E+00	1.24E−95
	Stdev	1.34E+03	3.91E+00	6.78E−94
	Best	1.14E+03	9.26E−01	7.00E−115
$F_3(x)$	Mean	9.47E+01	3.00E+01	4.55E−03
	Stdev	7.90E+01	1.76E+01	5.12E−03
	Best	7.62E+00	4.01E+00	2.41E−04
$F_4(x)$	Mean	5.64E−02	2.15E−01	2.51E−04
	Stdev	2.03E−02	7.24E−02	1.07E−04
	Best	1.92E−02	1.16E−01	6.28E−05

4. Results and Discussion

The proposed system consists of twenty PV modules linked in series for a maximum capacity of 3.082 kW and one wind turbine generator with a capacity of 1.4 kW. In grid-tied microgrid systems with battery banks, a 24V power converter is used. The BESS consists of four 6V batteries in series with a total voltage of 24V and a maximum capacity of 400Ah. This study presents optimum power flow management catering to the load profile requirement of microgrid assuming solar irradiance and wind speed values for a typical day. The fundamental assumption taken in the simulation is the residential consumers loading pattern will follow the estimated load data considered in this work and the solar and wind power generation will be as per the assumed irradiance and wind speed data based on historical records. The proposed system simulation is studied using MATLAB software in a PC having Intel i7 processor. The multiprocessing and complex nonlinear optimization solving capability of MATLAB helps in obtaining the results of accurate implementable strategy for the microgrid energy operation.

Table 5 shows the results of simulations that follow the ARO optimization technique for both Tier 1 (fixed price) and Tier 2 (TOU pricing). These numerical results illustrate the schedule of state-of-charge, battery voltage, and battery current.

Table 5. Cash flow for Tier 1 and 2 pricing

Case	Cash flow (CF) for a day in Rs.
Tier 1	14.91
Tier 2	33.57

Table 5 compares the daily profit of consumer for the Tier 2 TOU pricing with the fixed price. Tier 2's Cash Flow (CF) yields a greater profit.

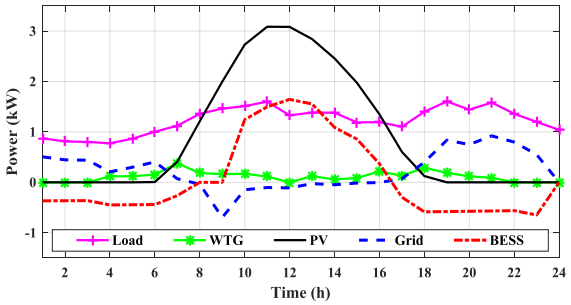

Figure 6. Active power profile in a day (Tier 1)

The profile of power sharing of the various entities on a typical day is shown in Figures 6 and 7 for Fixed price and TOU electricity pricing, respectively. In Figures 6 and 7, positive battery power represents a battery that is being charged, while negative battery power indicates a battery that is being discharged. Power consumption is represented by a positive value for grid power, power input by a negative value, and power consumption by a positive value for load power.

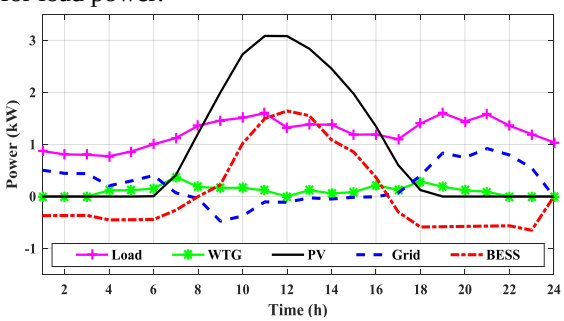

Figure 7. Active power profile in a day (Tier 2)

During a typical day for Tier 1 in Fig.8, the BESS is discharged during 12.00 AM to 7.00 AM. From 7.00 AM to 9.00 AM, it remains in rest condition as PV, wind, and grid supplies power to load. Then, the battery starts charging between 9.00 AM and 4.00 PM from solar power. The BESS is discharged during 4.00 PM to 11.00 PM to limit the power purchased from grid. The BESS is discharged until it reaches state of charge of 50%. The SOC of BESS remains constant from 11.00 PM to 12.00 AM. The user was getting a profit of 14.91 Rs. from the system.

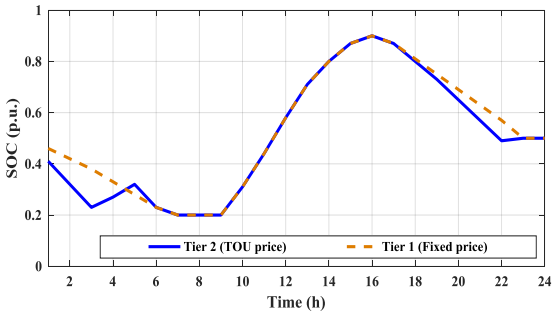

Figure 8. SOC schedule of BESS in a day

During a typical day for Tier 2 in Figure 8, the battery rapidly changes from discharging condition to charging condition and from charging condition to discharging condition to balance the demand on load side until it reaches state of charge of 20% from 12.00 PM to 7.00 PM. Then, the SOC remains constant from 7.00 AM to 9.00 AM. The BESS is charged during 9.00 AM to 4.00 PM with solar PV and it is discharged during 4.00 PM to 10.00 PM until it comes back to terminal SOC of 50% to offset the load. The SOC stays constant during 10.00 PM to 12.00 AM. The user gets the profit of Rs. 33.57 from the system.

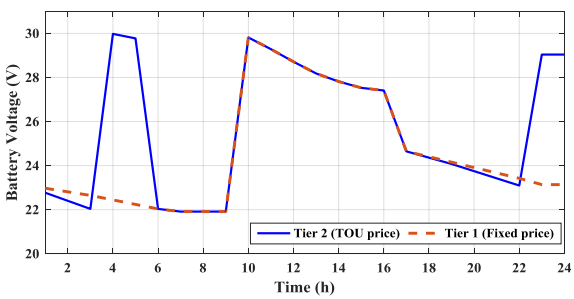

Figure 9. Voltage of the Battery in a day

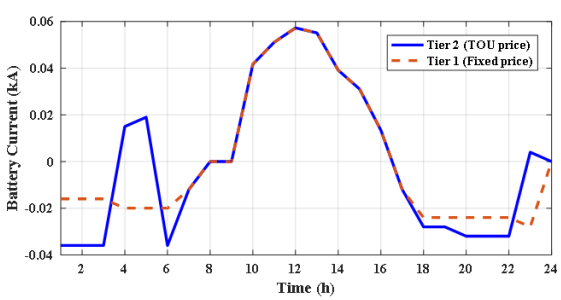

Figure 10. Current of the Battery in a day

Figures 9 and 10 show voltage and current flow of the battery storage in a day for Tier 1 and 2 pricing strategy. The floating voltage of the BESS varies within 22 V and 30 V and the variations in battery current are within 0.06 kA. The sign of the battery

current indicates charging and discharging of the battery.

5. Conclusions

This study demonstrates a novel method for optimizing system economics. The suggested system optimizes using the ARO algorithm. It comprises energy storage conditions and system-specific limitations. The PV/Wind/BESS combination provides the benefits of demand charge control, renewable energy time shifting, and capacity farming. Using the recommended strategy is noticed to enhance the cost savings. The suggested approach considers the fixed and time-of-use tariffs and determines SOC for each hour of the day in order to minimize the goal function considering state of health simultaneously. Several criteria are varied to evaluate the performance of the proposed system. The simulation is done utilizing Bhubaneswar, India's real-time irradiation and wind data. The results demonstrate the technological and financial benefits of integrating PV panels, WTG with BESS. The future scope of work can be extended to analyses the impact of electric vehicle integrated microgrid and optimal charging and discharging strategy. The effect of distribution transformer ageing can also be analysed for improving the life span and extending investment deferral period.

Nomenclature

Subscripts

ARO	Artificial rabbit optimisation
BESS	Battery energy storage system
CF	Cash flow
CS	Cuckoo search
DE	Differential evolution
EGP	Electricity grid price
EMS	Energy management system
FIT	Feed-in tariff
GSA	Gravitational search algorithm
IMD	Indian meteorological department
MILP	Mixed integer linear programming
MW	Molecular weight
PSO	Particle swarm optimization
PV	Photovoltaic
RES	Renewable energy sources
SOC	State of charge
SOH	State of health
TLBO	Teaching-learning-based optimization
TOU	Time of use
WTG	Wind turbine generation

Parameters and variables

$\mathrm{A(t)}$	Energy factor
BiC	Investment cost of BESS
BrC	Ageing cost of BESS
C_P	Cash inflow
C_r	Reference capacity of the battery
C_R	Cash outflow
I_{bat}	Current of the battery
η_{conv}	Converter efficiency
η_{wd}	Wind turbine efficiency
N_{bat}	Number of batteries connected in series
N_w	Number of wind turbines
$\mathrm{P\{A(t)\}}$	Probability of energy factor
P_{Grid}	Power received from grid
P_{Load}	Power supplied to load
P_{PV}	Power generated by a PV panel
$P_{rated_{PV}}$	Rated power of each PV panel
P_{bat}	Power supplied to battery
ρ	Density of air
R	Solar irradiance
R_C	Irradiance at a fixed radiation point
R_{STD}	Irradiance under standard condition
P_{WTG}	Power generated by wind turbine
V_{bat}	Voltage of the battery
v_{cin}	Cut-in speed of wind turbine
v_{cout}	Cut-out speed of wind turbine
v_{rd}	Rated speed of wind turbine
$\overrightarrow{\mathrm{x_i}}$	Position of individual rabbit in optimisation
Z	Ageing coefficient

References

1. Elavarasan, R.M., et al., SWOT analysis: A framework for comprehensive evaluation of drivers and barriers for renewable energy development in significant countries. Energy Reports, 2020. **6**: p. 1838-1864.
2. Solaun, K. and E. Cerdá, Climate change impacts on renewable energy generation. A review of quantitative projections. Renewable and sustainable energy Reviews, 2019. **116**: p. 109415.
3. Sarwar, M., et al., Optimal selection of renewable energy–based microgrid for sustainable energy supply. International Journal of Energy Research, 2022. **46**(5): p. 5828-5846.
4. Blesslin, S.T., et al., Microgrid optimization and integration of renewable energy resources: innovation, challenges and prospects. Integration of Renewable Energy Sources with Smart Grid, 2021: p. 239-262.

5. Ishaq, S., et al., A review on recent developments in control and optimization of micro grids. Energy Reports, 2022. **8**: p. 4085-4103.
6. Kumar, G.B., et al., Large scale renewable energy integration: Issues and solutions. Energies, 2019. **12**(10): p. 1996.
7. Shahgholian, G., A brief review on microgrids: Operation, applications, modeling, and control. International Transactions on Electrical Energy Systems, 2021. **31**(6): p. e12885.
8. Jabalameli, N. and A. Ghosh, Online centralized coordination of charging and phase switching of PEVs in unbalanced LV networks with high PV penetrations. IEEE Systems Journal, 2020. **15**(1): p. 1015-1025.
9. Kandari, R., N. Neeraj, and A. Micallef, Review on Recent Strategies for Integrating Energy Storage Systems in Microgrids. Energies, 2022. **16**(1): p. 317.
10. Zarei, A. and N. Ghaffarzadeh, Optimal Demand Response-based AC OPF Over Smart Grid Platform Considering Solar and Wind Power Plants and ESSs with Short-term Load Forecasts using LSTM. Journal of Solar Energy Research, 2023. **8**(2): p. 1367-1379.
11. Mirzakhani, A. and I. Pishkar, Finding the best configuration of an off-grid PV-Wind-Fuel cell system with battery and generator backup: a remote house in Iran. Journal of Solar Energy Research, 2023. **8**(2): p. 1380-1392.
12. Aryan Nezhad, M., Economic Impacts of Long-Term Wind Speed Changes on Optimal Planning of a Hybrid Renewable Energy System (HRES). Journal of Solar Energy Research, 2021. **6**(1): p. 656-663.
13. Ghaffarzadeh, N. and H. Faramarzi, Optimal Solar plant placement using holomorphic embedded power Flow Considering the clustering technique in uncertainty analysis. Journal of Solar Energy Research, 2022. **7**(1): p. 997-1007.
14. Theo, W.L., et al., An MILP model for cost-optimal planning of an on-grid hybrid power system for an eco-industrial park. Energy, 2016. **116**: p. 1423-1441.
15. Logesh, R., Resources, configurations, and soft computing techniques for power management and control of PV/wind hybrid system. Renewable and Sustainable Energy Reviews, 2017. **69**: p. 129-143.
16. Fathima, A.H. and K. Palanisamy, Optimization in microgrids with hybrid energy systems–A review. Renewable and Sustainable Energy Reviews, 2015. **45**: p. 431-446.
17. Gamarra, C. and J.M. Guerrero, Computational optimization techniques applied to microgrids planning: A review. Renewable and Sustainable Energy Reviews, 2015. **48**: p. 413-424.
18. Sarker, M.R., et al., Optimal operation of a battery energy storage system: Trade-off between grid economics and storage health. Electric Power Systems Research, 2017. **152**: p. 342-349.
19. Parvin, K., et al., The future energy internet for utility energy service and demand-side management in smart grid: Current practices, challenges and future directions. Sustainable Energy Technologies and Assessments, 2022. **53**: p. 102648.
20. Khezri, R. and A. Mahmoudi, Review on the state‐of‐the‐art multi‐objective optimisation of hybrid standalone/grid‐connected energy systems. IET Generation, Transmission & Distribution, 2020. **14**(20): p. 4285-4300.
21. Patnaik, S., M.R. Nayak, and M. Viswavandya, Optimal Battery Energy Storage System Management with Wind Turbine Generator in Unbalanced Low Power Distribution System. Advances in Electrical and Electronic Engineering, 2023. **20**(4): p. 523-536.
22. Kunya, A.B., A.S. Abubakar, and S.S. Yusuf, Review of economic dispatch in multi-area power system: State-of-the-art and future prospective. Electric Power Systems Research, 2023. **217**: p. 109089.
23. Zeng, B., et al., Optimal demand response resource exploitation for efficient accommodation of renewable energy sources in multi-energy systems considering correlated uncertainties. Journal of Cleaner Production, 2021. **288**: p. 125666.
24. Chen, H., L. Gao, and Z. Zhang, Multi-objective optimal scheduling of a microgrid with uncertainties of renewable power generation considering user satisfaction. International Journal of Electrical Power & Energy Systems, 2021. **131**: p. 107142.
25. Jordehi, A.R., Optimisation of demand response in electric power systems, a review. Renewable and sustainable energy reviews, 2019. **103**: p. 308-319.
26. Tian, Y., et al., Evolutionary large-scale multi-objective optimization: A survey. ACM Computing Surveys (CSUR), 2021. **54**(8): p. 1-34.
27. Adam, S.P., et al., No free lunch theorem: A review. Approximation and Optimization:

Algorithms, Complexity and Applications, 2019: p. 57-82.
28. Rodríguez-Molina, A., et al., Multi-objective meta-heuristic optimization in intelligent control: A survey on the controller tuning problem. Applied Soft Computing, 2020. **93**: p. 106342.
29. Wang, L., et al., Artificial rabbits optimization: A new bio-inspired meta-heuristic algorithm for solving engineering optimization problems. Engineering Applications of Artificial Intelligence, 2022. **114**: p. 105082.
30. de Siqueira, L.M.S. and W. Peng, Control strategy to smooth wind power output using battery energy storage system: A review. Journal of Energy Storage, 2021. **35**: p. 102252.
31. Yang, Y., et al., Battery energy storage system size determination in renewable energy systems: A review. Renewable and Sustainable Energy Reviews, 2018. **91**: p. 109-125.
32. Nayak, C.K. and M.R. Nayak, Technoeconomic analysis of a grid-connected PV and battery energy storagesystem considering time of use pricing. Turkish Journal of Electrical Engineering and Computer Sciences, 2018. **26**(1): p. 318-329.
33. Nayak, C.K., K. Kasturi, and M.R. Nayak, Economical management of microgrid for optimal participation in electricity market. Journal of Energy Storage, 2019. **21**: p. 657-664.
34. Yazdanpanah Jahromi, M.A., S. Farahat, and S.M. Barakati, Optimal size and cost analysis of stand-alone hybrid wind/photovoltaic power-generation systems. Civil Engineering and Environmental Systems, 2014. **31**(4): p. 283-303.
35. Batteries, R.F.D.C., S-550 Spec 01. Springfield: Rolls Battery Co., 2001. 2020.
36. Lemaire-Potteau, E., et al. Assessment of storage ageing in different types of PV systems technical and economical aspects. in 23rd European Photovoltaic Solar Energy Conference (Valencia, Spain, 2008). 2008.
37. Delaille, A., Development of New State-of-Charge and State-of-Health Criteria for Batteries Used in Photovoltaic Systems University Pierre et Marie Curie. Ph. D Report (French), 2006.
38. Guo, Y., et al., Failure modes of valve-regulated lead-acid batteries for electric bicycle applications in deep discharge. Journal of power sources, 2009. **191**(1): p. 127-133.
39. Bhoi, S.K. and M.R. Nayak, Optimal scheduling of battery storage with grid tied PV systems for trade-off between consumer energy cost and storage health. Microprocessors and Microsystems, 2020. **79**: p. 103274.